Progress In Electromagnetics Research M, Vol. 47, 45–55, 2016

An Efficient Analysis on the Fitting Error Caused by the Deformation of Metal Pylon in the RCS Measurement

Da-Wei An* **and Wu-Yi Chen**

Abstract—Target-supporting metal pylon predominantly contributes to background scattering in radar cross section measurement. The separation of scattering from the target and background demands stable background scattering. However, target translation creates variations in metal pylon deformation and changes its scattering, which yields errors in background separation. Analyzing the relationship between the structural parameters of metal pylon and the error caused by its deformation is necessary to reduce errors. A simplified mapping of the relationship is deduced according to the mechanical and electromagnetic theories involved. The approach combines geometrical theory of diffraction for pylon scattering and numerical integration in calculating the deflection of metal pylon to determine the variation of metal pylon scattering, and calculates error in the circle fitting caused by the variation. Simulations with commercial software are employed to verify the efficiency of the numerical model. Although it is slightly contaminated by target-pylon interaction, the approach is 800 times faster than the software simulation. An example of optimization and analysis is provided to demonstrate the trends of optimum structural parameters and fitting error within different pylon weight limits. Such an example proves that the approach can overcome the deficiency of traditional analysis which separately assesses the mechanical and RCS performances of metal pylon.

1. INTRODUCTION

In radar cross section (RCS) measurements within test ranges, a metal pylon is a kind of target support structure often used to avoid target-ground interaction and set the target in the quiet zone [1]. A canonical metal pylon is shaped like a forward-swept wing and inclines toward the incidence direction of the test plane wave. The cross section of a metal pylon is usually ogive, although other sections with a small wedge angle of the leading edge are also used. Traditionally, a two-axis rotator is mounted on top of the pylon to change target posture, and the target must be modified to fit the rotator exactly. Therefore, the target is mounted on top of the pylon and the rotator is concealed by the target during measurements. The target can change its azimuth and pitch angles through the rotator motion to expand the test pose. Some new rotators can also provide the target with a translation movement parallel to the direction of the plane wave, for separating the echo signal of the target from the background signal by circle fitting of the measured data [2–4].

The raw measured echo signals combine the scattering of the target and background, including the metal pylon. Therefore, background scattering should be small to reduce its influence on measurement error. Furthermore, the background signal can be separated from the raw measured signals by several approaches with multiple measurements, demanding that the background scattering is kept stable during the course for accurate separation. The metal pylon is the only object illuminated by radar wave apart from the target in the same zone, and its scattering signal cannot be eliminated by the range gate. Thus, it is assumed to be the dominant source of background scattering. According to the aforementioned demands of background scattering, the metal pylon should possess low RCS and small

Received 11 January 2016, Accepted 14 March 2016, Scheduled 22 March 2016
* Corresponding author: Da-Wei An (sarlatin@163.com).
The authors are with the School of Mechanical Engineering and Automation, Beihang University, Beijing, China.

deformation features during measurements because deformation changes both the amplitude and phase of its electromagnetic scattering. A metal pylon is sometimes used to carry a heavy target of up to 20,000 kg [5], and the working frequency can be higher than 18 GHz [6]. Thus, the deformation may be significant compared with the wavelength, and the variation in complex scattering signals by the metal pylon cannot be ignored as it contributes to the measurement error. On the other hand, the metal pylon might not be the only target support structure in a test range and should be conveniently moved away to allow other positioners or supporters to move in. For security considerations, some metal pylons should be retractable. They require that the weight of the metal pylon should be as light as possible, which is in conflict with the stiffness requirement and could increase the deformation of the metal pylon.

Pylon RCS, deformation, and weight are determined by structural parameters, and their demands on the structural parameters may be in conflict with one another. Published studies on metal pylon focused on either electromagnetic or mechanical field. The relationships between the structural parameters of the metal pylon and its RCS were investigated by Knott [7], and Lai and Burnside [8]. Some studies on the mechanical design of metal pylon have been published, including the bionic design for high strength-to-weight ratio [9]. However, some low-RCS configurations, such as small wedge angle, narrow cross section, and small tilt angle, are against the high stiffness demand. Increasing the thickness and size of the cross section of the pylon structure can reduce pylon deformation but results in the heavy weight. The larger cross section can also lead to higher RCS. In summary, an optimum design of the metal pylon should contain comprehensive considerations covering both the electromagnetic and mechanical fields. However, no research has integrally analyzed the relationship between measurement error and such design objectives as low RCS, high strength, and light weight. Furthermore, metal pylons in different test ranges usually require different quiet zone heights, target loads, working frequencies, and possibly other customer needs. Every metal pylon requires unique optimization of the structural parameters to ensure its best performance. Thus, analysis of the relationship between the structural parameters and their contribution to measurement error should be flexible and fast. Simulation in the commercial software can accurately calculate the aforementioned contribution to measurement error, but it is time consuming. Consequently, a simple and effective approach is preferred to assess the relationship between the structural parameters of the metal pylon and the measurement error caused by pylon deformation according to the mechanical and electromagnetic theories involved. The approach can then be used to obtain the optimum design of metal pylon.

2. SIMPLIFIED MAPPING OF THE RELATIONSHIP

2.1. Applicable Conditions

The analysis is simplified based on the following conditions. In RCS measurements, complex scattering signals including the target and background are separated by the method introduced in [2–4], which utilizes multiple measurements during target translation along the direction of the incidence plane wave and circle fitting to process the raw measured data. The inner structure of the metal pylon is simplified as a hollow one with uniform wall thickness and is manufactured using a single homogenous material. The height of the metal pylon is determined by the test range size and the difference between the tilt angles of the leading edge, and the trailing edge is 10° in most existing designs, so that they are constant in the analysis. The variables of the metal pylon to be analyzed can be reduced as tilt angle, shape and length-to-width ratio of the horizontal cross section, and thickness of the structural wall.

The analysis focuses on the mechanical structural parameters, thus, it evaluates pylon with a metallic surface without any absorbing materials, given that commercial low-RCS metal pylons usually exhibit a metallic surface quality and leading edge sharpness [5, 6]. The target-pylon interaction of electromagnetic scattering is uncertain and varies with different types of targets [7, 10]. The interaction is usually reduced either by absorbing materials coated on the bottom of the rotator and the top of the metal pylon or by post-processing of the measurement data [11], rather than the optimum structural parameters of the metal pylon. Thus, the interaction is ignored to simplify the process. Indeed, the effect of the interaction on the error resulting from pylon deformation is negligible, and will be discussed later in this paper.

Given that the metal pylon has a small horizontal cross section compared with its height, it exhibits higher RCS in vertical polarization than in horizontal polarization (usually more than 10 dB). Therefore,

it contributes larger measurement errors in the vertical polarization. So the simplified analysis focuses on vertical polarization. Metal pylon is employed for measurements at high frequencies because it exhibits low RCS in this case. Therefore, the analysis only considers high frequencies in which the pylon size is electrically large and the high-frequency asymptotic methods are appropriate to calculate the RCS of metal pylon. Usually the working frequency of metal pylons is higher than 1 GHz.

2.2. Mechanism of the Circle-Fitting Error Caused by Metal Pylon Deformation

When using a coherent radar in RCS measurement, the measured signals, including the target and pylon, result in complex data. The phase of the scattered electric field of the target changes as the target translates during the measurement. So the measured data trace a circle or an arc in the complex plane, whose radius represents the amplitude of the scattering electric field of the target, and the position of the center represents the scattering electric field of the background including the metal pylon [2]. Notably, the method demands the background signal be basically stable during measurement to ensure that the center of the complex circle does not translate significantly for circle-fitting accuracy.

Reference [2] used the aforementioned method to measure a low-RCS target at 2.8 GHz, when the background and target RCS were of the same magnitude, and the target was a light weight arrow model. If the test target is heavy, the load status before and after translation will exhibit an evident difference. Therefore, the variation in the deformation of the pylon in the course is significant with respect to wavelength at high frequencies, and the phase of pylon scattering varies visibly. The deformation also changes the amplitude of pylon scattering. Thus, the vector of the scattered field of metal pylon shifts in the course of multiple measurements. Overall, if the RCS magnitude of a heavy test target is not higher than the metal pylon in a high-frequency measurement, shifting of the scattered field vector by the metal pylon cannot be ignored compared with the amplitude of the scattered field by the test target.

In a complex plane, it means that the center of the complex circle translates visibly compared with the radius. Thus, the practical complex data cannot strictly trace a circle or an arc, and the regression radius obtained by circle fitting based on the data produces a difference from the ideal value, which is the error. In Fig. 1, σ_{P1} and σ_{P2} represent the pylon RCS in two deformation statuses. D_C is the corresponding shift distance of the circle center. The detailed relationship between them is discussed in Section 2.3. The aforementioned mechanisms indicate that the error comes from the mixed contributions of RCS and the deformation of metal pylon.

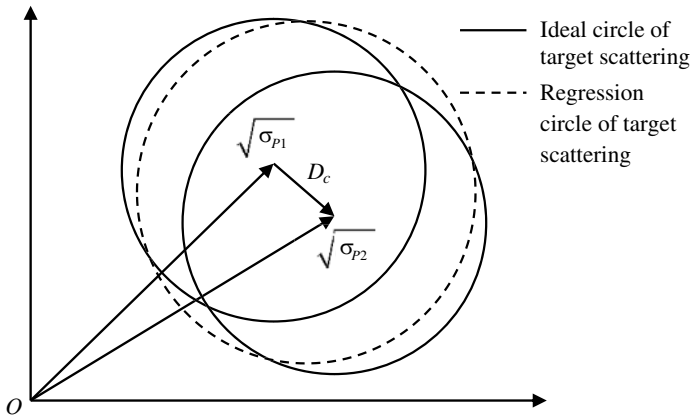

Figure 1. Error in circle fitting caused by pylon deformation.

2.3. Construction of Simplified Mapping

According to the above mechanism, a simplified relationship can be deduced between the circle-fitting error caused by the pylon deformation and the structural parameters of the metal pylon along with the measurement conditions including target weight, target RCS, translation range and measurement

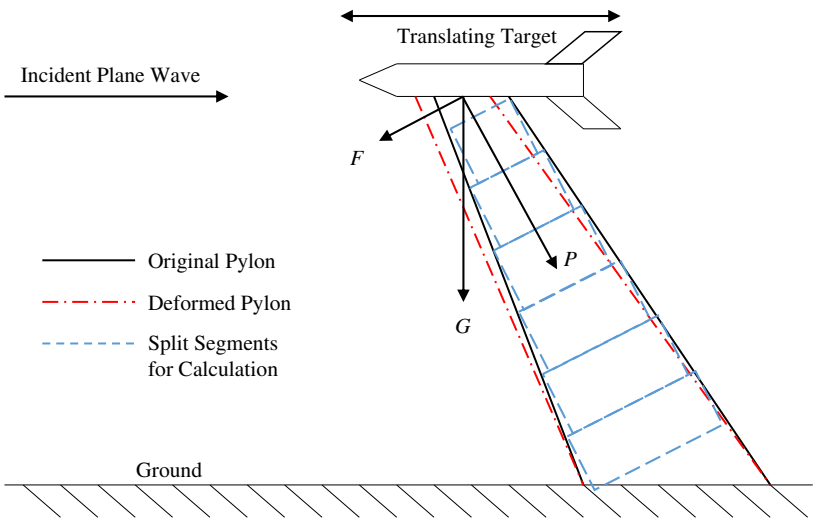

Figure 2. Translating target measured on metal pylon and sketch of the split pylon for deflection calculation.

frequency. The mapping can be used in the effective analysis and design of the structural parameters of metal pylon.

First, we calculate the variation in metal pylon deformation in the measurement. The target load can be simplified as concentrated force G and additional moment M when the target translates from the original position. G can be resolved into lateral force F and axial force P. P yields a slight axial deformation of the pylon which can be ignored. Metal pylon can be treated as a continuous beam with varying cross sections. F and M determine the deflection, W. W can be calculated through numerical integration by splitting the pylon into many uniform section segments, as shown in Fig. 2.

The contribution of a single segment to total deflection W can be easily calculated according to the following formulas of uniform section cantilever beam deflection:

$$w_{i1} = F\frac{(L/n)^3}{3EI_i} + M_i\frac{(L/n)^2}{2EI_i} \tag{1}$$

$$\mu_i = F\frac{(L/n)^2}{2EI_i} + M_i\frac{L/n}{EI_i} \tag{2}$$

where w_{i1} is the direct contribution to total deflection, μ_i the bending angle of the ith segment, L the length of the pylon along its central line, n the number of total segments, E the elastic modulus of the pylon material, I_i the moment of inertia of the ith segment that can be calculated according to the cross section size, and M_i the moment that acts on the ith segment, which can be calculated as follows:

$$M_i = FL(1 - i/n) + M \tag{3}$$

The contribution of bending angle to the deflection of a single segment can be approximated as a linear superposition, which is given as:

$$w_{i2} = (L/n)\sum_{j}^{i-1}\mu_j \quad (i = 2, 3, \ldots, n) \tag{4}$$

When $i = 1$, bending angle has no contribution to the deflection, so $w_{12} = 0$. The deflection at the end of the ith segment is:

$$W_i = \sum_{j=1}^{i}(w_{j1} + w_{j2}) \tag{5}$$

Then, $W = W_n$.

Second, we calculate the variation in the pylon scattering vector caused by deformation. According to reference [7], in theory, the principal contribution of backscattering by the metal pylon working in high frequencies is diffraction on the leading edge. In practice, however, creeping wave may be another relatively significant source of backscattering in high frequencies. The side surfaces of the metal pylon are approximately perpendicular to the ground, so the contribution of creeping wave to backscattering is significant in horizontal polarization but can be ignored in vertical polarization. As the simplified analysis focuses on vertical polarization, the RCS of metal pylon can be regarded as the diffraction on the leading edge in high frequencies. A method based on geometrical theory of diffraction (GTD) can be used to estimate the scattering on the leading edge [12]. In vertical polarization, the prediction is expressed as follows:

$$\sigma = \frac{1}{\pi f^2}\left[\frac{c}{(2-\beta/\pi)\,\pi\cot\tau\sin\left(\pi/\left(2-\beta/\pi\right)\right)}\right]^2 \tag{6}$$

where f is the plane wave frequency, c the speed of light, β the interior wedge angle of the leading edge, and τ the tilt angle of the leading edge with respect to the ground. Note that Eq. (6) is independent of the length of the pylon and σ is the maximum value of the scattered field by the pylons with the same tilt angle and wedge angle but different lengths. The more accurate prediction of diffraction involves a trigonometric function that includes the leading edge length, f and τ [7]. Therefore, these three variables cause the actual diffraction to fluctuate between null and the result of Eq. (6) without constant periodicity. A metal pylon works in a wide range of frequencies. Different leading edge lengths and tilt angles in the design will be analyzed to reduce the circle-fitting error. For simplification and design margin, we primarily concern with the peak value calculated by Eq. (6).

The metal pylon usually possesses a small horizontal cross section in relation to its height. Thus, we can ignore the deformation of horizontal cross sections and assume that the deflection of the pylon leading edge and that of the central line are the same. The deflection of the leading edge is also referred to as W. Deflection brings changes to the tilt angle. According to Eq. (6), the amplitude of the scattered electric field by the metal pylon varies. In practice, the upper portion of the pylon predominantly contributes to deflection, and only the upper portion is exposed in the quiet zone, generating most of the measurable electromagnetic scattering. Consequently, we can simplify calculation by focusing on the variation in tilt angle and scattering of the upper portion of the metal pylon in the quiet zone. The component of W along the direction of the incidence wave is:

$$W_x = W\sin\tau_C \tag{7}$$

where τ_C is the tilt angle of the central line of the pylon. Equation (6) only works when the leading edge is straight, whereas the practical deformed edge is curved. However, the deflection is very small compared with the length of the metal pylon in the quiet zone, so the deformed edge can be simplified as straight to utilize Eq. (6) without significant error. According to the geometrical relationship shown in Fig. 3, the tilt angle of the deformed leading edge τ_{def} is:

$$\tau_{def} = \arctan\left(L_{\mathit{eff}}\sin\tau/\left(L_{\mathit{eff}}\cos\tau + W_x - W_{\text{bottom}}\sin\tau_c\right)\right) \tag{8}$$

where L_{eff} is the length of the metal pylon in the quiet zone, and W_{bottom} is the deflection of the metal pylon at the bottom of the quiet zone. If the kth segment is the bottom segment in the quiet zone, it can be simplified as $W_{\text{bottom}} = W_k$. Replacing τ with τ_{def} in Eq. (6), the RCS of the deformed portion illuminated in the quiet zone can be calculated.

The deformation also causes a varied scattering phase of the metal pylon. The portion of the pylon in the quiet zone can be considered to have an average displacement D_P along the direction of the incidence wave, which is:

$$D_p = \frac{1}{n-k+1}\sum_{k}^{n} W_i\sin\tau_C \tag{9}$$

The phase of the complex electric field shifts 2π when the object moves for a distance of $\lambda/2$ in the test range, where λ is the radar wavelength. So the variation of the phase is:

$$\Delta\phi = 4\pi D_P/\lambda \tag{10}$$

Since we obtain the variation in the amplitude and phase of pylon scattering, the translation distance of the circle center can be easily calculated, labeled as D_C in Fig. 1. When the incident electric

field is the unit amplitude, the RCS is proportional to the square of the scattered electric field of the object. Therefore, if we donate the RCS of the metal pylon and target as σ_P and σ_T, we can use $\sqrt{\sigma_P}$ and $\sqrt{\sigma_T}$ instead of the amplitude of their scattered electric field in the complex plane while maintaining the same proportion. In this case,

$$D_c = \sqrt{\sigma_{P1} + \sigma_{P2} - 2\sqrt{\sigma_{P1}\sigma_{P2}}\cos\Delta\phi} \tag{11}$$

where σ_{P1} and σ_{P2} are the pylon RCS corresponding to the deformed pylon before and after target translation.

Finally, we calculate the error in circle fitting caused by center shift. A series of points is created as (x_i, y_i) to simulate the measured raw signals including the target and metal pylon:

$$x_i = \cos\left(\frac{4i\pi D_T}{n\lambda}\right)\sqrt{\sigma_T} + \frac{iD_C}{n}\cos\alpha \tag{12}$$

$$y_i = \sin\left(\frac{4i\pi D_T}{n\lambda}\right)\sqrt{\sigma_T} + \frac{iD_C}{n}\sin\alpha \tag{13}$$

The trace of (x_i, y_i) rotates around the center with the radius of $\sqrt{\sigma_T}$, whereas the center moves within a distance of D_C. D_T is the stroke of physical translation of the target along the incident direction of the plane wave. The phase difference between the scattering of the pylon and target is uncertain with different targets and other measurement conditions. Thus, we add α to change the phase of D_c to simulate the variation in phase difference. The points are processed by the circle-fitting method to derive the fitted radius R_{fit}. The error between the regression radius and the ideal radius can be expressed as:

$$\varepsilon = \left|R_{fit} - \sqrt{\sigma_T}\right| / \sqrt{\sigma_T} \tag{14}$$

The error varies when α changes. We should change α in the range of $(0, 2\pi)$ to derive the maximum value as the final error for the design margin. All the equations and procedures presented in this section form the simplification mapping, which can be contracted as:

$$\varepsilon = F(X) \tag{15}$$

where X is a series of variables describing the structural parameters of the metal pylon. The other measurement conditions can be considered as the components of mapping.

3. VERIFICATION BY SIMULATION

3.1. Simulation Configuration

A number of commercial simulation software platforms are used to verify the effectiveness of simplified mapping. The 3D geometric models of hollow pylons are created using CAITA V5 r20 [13], and

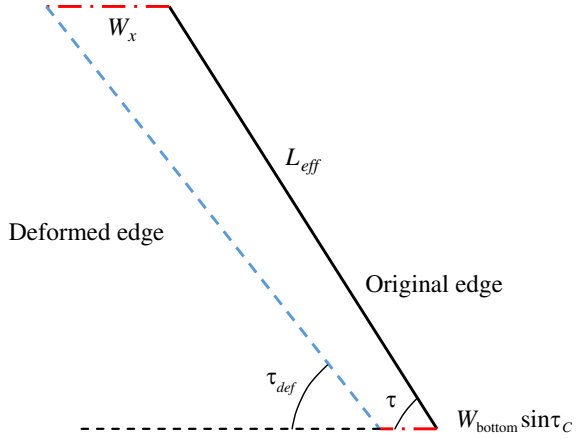

Figure 3. Relationship between geometries before and after deflection.

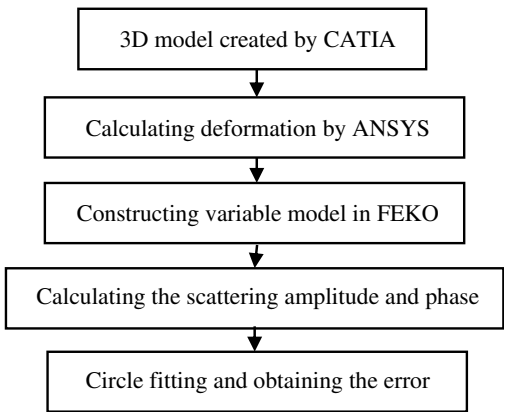

Figure 4. Simulation process.

are transferred to ANSYS 14.5 [14] to calculate the deformations. The deformation data are used to set up the parametric pylon model in FEKO 6.0 [15] to simulate pylon deformation during RCS measurement and calculate the electromagnetic scattering including the translating target and deformed pylon. Finally, the simulation results of the amplitude and phase from FEKO are processed by circle fitting. The detailed procedures are introduced in reference [16] and can be depicted as a flowchart in Fig. 4. The basic structural sizes of the metal pylon in the simulation are shown in Fig. 5, and the RCS of the target used to calculate the relative error is set as −30 dB. Different wall thicknesses (5, 7.5, and 10 mm) and target weights (1000, 2000, and 3000 kg) are used as the variables in the simulations. The above simulation is performed under the frequency of 1 GHz. Another set of simulations whose frequencies are extend to 1, 2, 2.7, and 4 GHz is carried out, focusing on the status with 1000 kg target load and 5 mm wall thickness. Translation range is modified according to the frequency to hold the phase shift of target. Note that there will be strong coupling at 3 GHz because the wavelength matches the length of the top of the pylon model. Thus, 2.7 GHz is employed instead of 3 GHz to prevent such coupling.

The solver used in FEKO is the method of moments (MoM). Other solvers in FEKO are not suitable in this study. The multilevel fast multipole method (MLFMM) is a more effective solver than MoM, but its error from convergence residuum is only acceptable when calculating static RCS. However, we utilize FEKO to calculate the dynamic variation in pylon RCS during deformation, whose magnitude is no more than the millivolts level in electric field amplitude. Thus, the error of MLFMM may lead to significant contamination and failure in circle fitting. The asymptotic solvers of FEKO also have limitations in solving the problem. The physical optics (PO) solver and the uniform theory of diffraction (UTD) solver in FEKO can only calculate the diffraction of a straight wedge formed by two flat surfaces, so they fail in the ogive cross section. The geometrical optics (GO) solver in FEKO cannot consider the wedge diffraction [15]. Overall, only the MoM solver in FEKO can stably calculate the variation in pylon RCS and consider the diffraction of the leading edge properly. The MoM method requires an N^2 scaling of memory and N^3 in CPU time, when there are N basis functions that need to be solved. Simulations at higher frequencies demand more meshes of the pylon model and make N increase. Therefore, the upper limit of simulation frequencies is 4 GHz based on our computing resource. These models are also calculated by the simplified mapping, which is coded in Matlab.

3.2. Comparison and Analysis

The results of different load statuses at 1 GHz are shown in Fig. 6, in which the simulations do not consider the target-pylon interaction in electromagnetic scattering. The results of simplified mapping are 9.7% larger than those of simulation in average. The comparison of the two results at 1–4 GHz is shown in Fig. 7, demonstrating the performance of simplified mapping in higher frequencies. The

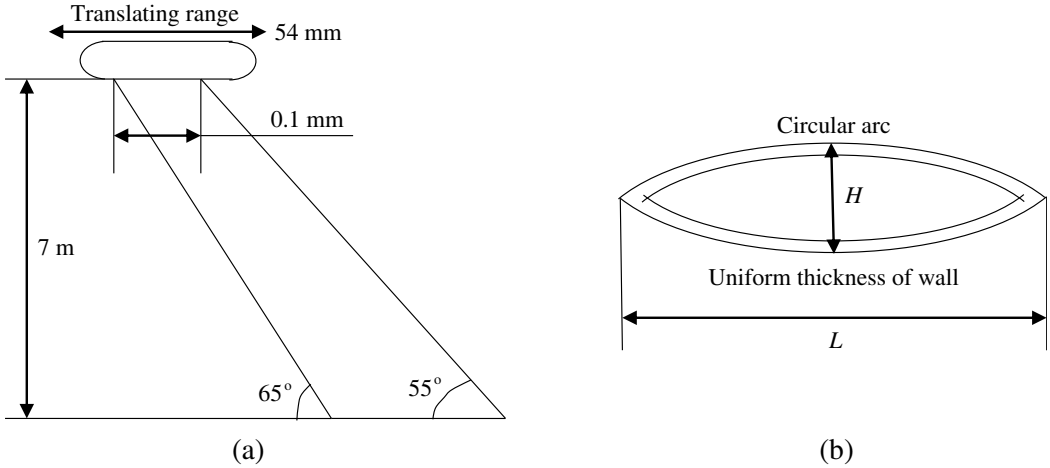

Figure 5. Structural parameters of the pylon model in the verification. (a) Side look. (b) $L : H = 4 : 1$.

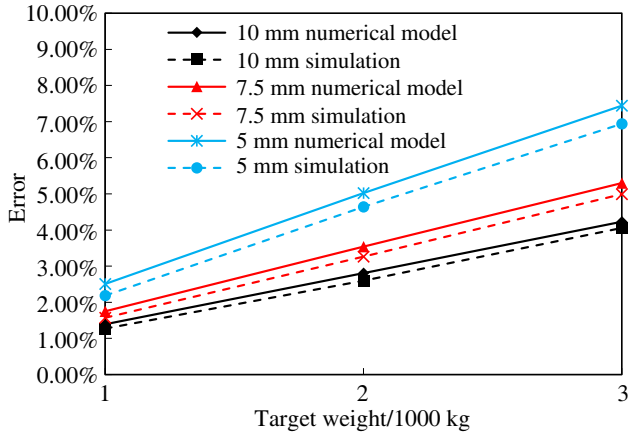

Figure 6. Comparison of errors calculated by the numerical model and simulation (the numbers in the legends donate the wall thickness).

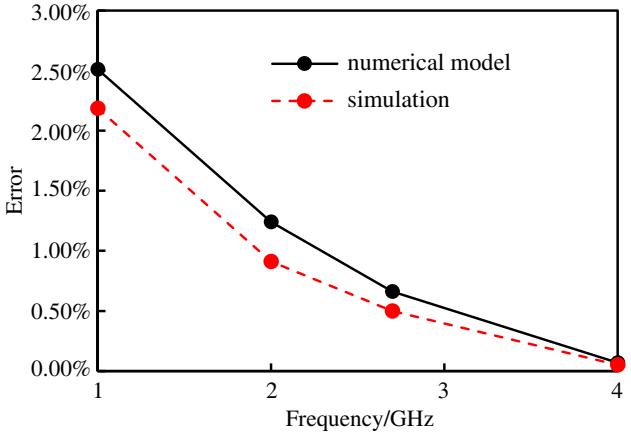

Figure 7. Comparison of the errors from 1 to 4 GHz (wall thickness is 5 mm and target load is 1000 kg).

circle-fitting error decreases as frequency increases. The results of simplified mapping always exceed the ones from simulations with an acceptable deviation.

The estimation of Eq. (6) is a sidelobe envelope of the possible RCS of metal pylons, and it may contribute to the primary error of simplified mapping. The comparison in Fig. 8 proves this conjecture. When using the pylon RCS simulated by FEKO instead of the estimation with Eq. (6) in the numerical model, the results are similar to those obtained by full simulation. To assess the influence of the target-pylon interaction on the results, Fig. 9 shows another simulation using a -35 dB half-ogive target flush-mounted on the pylon. In this simulation, we subtract the circle-fitting error with a rigid pylon model from that with a deforming pylon model to obtain the difference, which is the error affected by the target-pylon interaction. The result shows that the target-pylon interaction slightly contaminates the circle-fitting error from pylon deformation. Thus, neglecting the target-pylon interaction is reasonable.

The simplified mapping runs much faster than software simulation. The CPU time of a single result in Fig. 6 by the simplified mapping is 0.33 s, whereas that by software simulation is 269.85 s. Simplified mapping is 800 times faster than software simulation. When frequency increases, the cost of computing resource by electromagnetic simulation will increase exponentially, whereas the simplified mapping always requires a similar computing time since its computational complexity is independent of frequency. Furthermore, the above values are only the CPU time. As the simulation uses multiple software, data transfer between them and the model building requires additional time. Meanwhile, they are hard to process automatically. However, the mapping can be constructed as a single function, and it is easy to calculate repeatedly. In the analysis and optimization of metal pylon, plenty sets of variables are calculated to compare their circle-fitting errors. Therefore, full or single software simulation is not suitable in optimization, whereas simplified mapping is easy and efficient. For instance, the CPU time by FEKO of a single result in Fig. 6 is 157.25 s, so combining FEKO simulation will be much slower than the simplified mapping. More importantly, every single calculation in FEKO requires an individual pylon model created manually according to the corresponding deformation data, which makes the automatic optimization almost impossible.

The Verification is realized by commercial simulation software rather than by experiments for several reasons. First, commercial software, such as ANSYS or FEKO, possesses satisfying accuracy in analyzing this problem. Second, the simplified mapping is mainly used in the design but not in testing the actual pylon. Through simulation, we can easily verify the numerical model with different structure parameters of metal pylon and target loads. However, it is very difficult to manufacture so many pylons and targets just for experiments. Lastly, the simulation conditions are much easier to control than the experiment environments to avoid the interference from the relevant factors.

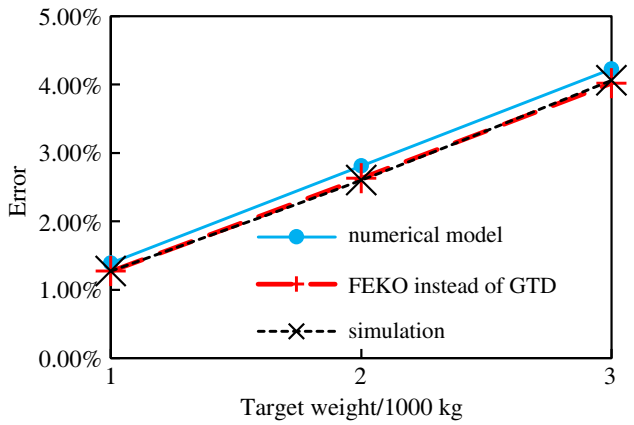

Figure 8. Deviation contributed by GTD (wall thickness is 10 mm).

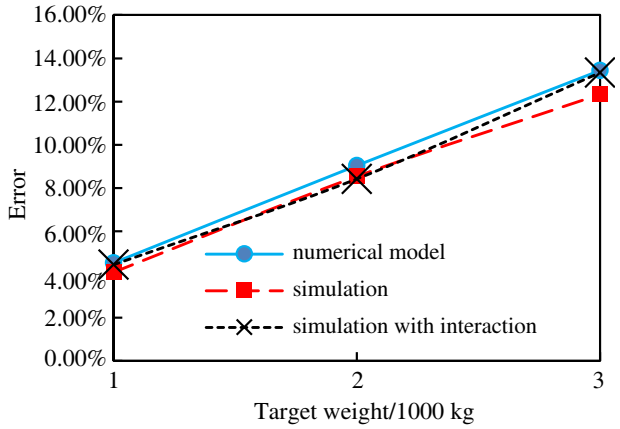

Figure 9. Comparison of error contaminated by the target-pylon interaction (wall thickness is 5 mm).

4. IMPLEMENTATION IN OPTIMIZATION AND ANALYSIS

An example of optimization is presented. The variables to be optimized are the structural parameters of a metal pylon. The simplified mapping is implemented as the objective function. The optimization results can be used to analyze the trends of structural parameters with different design demands.

Equation (15) is nonlinear, so that the Genetic Algorithm (GA) is selected as the optimization tool. Equation (15) is also the fitness function. The pylon weight is added as a constraint for lightweight design:

$$\rho V(X) \leq m_{MAX} \tag{16}$$

where ρ is the density of the pylon material, $V(X)$ the volume of the metal pylon calculated according to the structural parameters, and m_{MAX} the maximum weight of the metal pylon that is acceptable in the design. The goal of optimization is to derive the minimum value of the fitness function in Eq. (15). In the optimization, the height of the pylon is 7 m, the tilt angles of the leading edge and central line are fixed at 65° and 60°, the length of the top cross section is 200 mm, and the horizontal cross section is ogive. The approach can optimize the tilt angle, configuration of the cross section, and wall thickness of the metal pylon simultaneously, according to the construction of Eq. (15). In the example, only the wall thickness and length-to-width ratio of the cross section are the variables to be optimized to facilitate a clear demonstration. In the optimization, the maximum weight of the target is 3000 kg, and its RCS is −35 dB at 1 GHz.

Table 1. Example of optimization results.

Pylon weight limit/kg	Length-to-width ratio	Thickness/mm	Optimum error
1200	5.21	10.802	3.32%
1300	5.07	11.713	3.11%
1400	4.82	12.953	2.92%
1500	4.58	13.466	2.76%
1600	4.51	14.380	2.62%

Table 1 shows the optimum results with different pylon weight limits. The heavier the weight limit is, the smaller the circle-fitting error is achieved. When the weight limit increases, the optimum wall thickness increases to strengthen the stiffness of the metal pylon, but the horizontal cross section is wider, which opposes the low RCS configuration. The results prove that pylon deformation cannot be

ignored in the design of metal pylon for high frequency measurement accuracy. The analysis based on the simplified mapping can overcome the limitations of the pure RCS reduction design of metal pylon to obtain better performance in reducing measurement error, because the method is a comprehensive consideration that covers both the mechanical and electromagnetic factors.

5. CONCLUSION

An efficient analysis is introduced based on a simplified mapping relationship between metal pylon structural parameters and RCS measurement error caused by pylon deformation. This approach evaluates the measurement method using a translating target and circle-fitting post-process to separate the signals of the target and background.

The approach is an integrated analysis that combines the mechanical and electromagnetic fields. The appropriate approximation algorithm is utilized to make that its calculation is 800 times faster than the commercial software simulation. The verification by simulation indicates that the main deviation originates from the GTD prediction of pylon RCS. Moreover, the contamination of the target-pylon interaction is marginal in the circle-fitting error. The approach can simultaneously analyze and optimize the most important structural parameters of metal pylon.

An example of optimization and analysis using the GA method is given, which proves that the approach can provide better structural parameters than the traditional low-RCS design to reduce the final error because it considers pylon deformation.

Although no direct comparison is made between the calculated results and tested ones, the commercial software simulation can conveniently verify the approach in different parameters and conditions. The approach is used reliably in the optimum design of metal pylon. The metal pylons developed according to the method exhibit satisfactory performance in low RCS and high rigidity.

REFERENCES

1. Knott, E. F., J. Shaeffer, and M. Tuley, *Radar Cross Section*, 2nd Edition, SciTech Publishing, New York, 2004.
2. Muth, L. A., C. M. Wang, and T. Conn, "Robust separation of background and target signals in radar cross section measurements," *IEEE Trans. Instrum. Meas.*, Vol. 54, No. 6, 2462–2468, 2005.
3. Xu, X.-J., "A background and target signal separation technique for exact RCS measurement," *International Conference on Electromagnetics in Advanced Applications (ICEAA)*, 891–894, 2012.
4. Zhao, J.-C. and M. Lv, "Using Kasa method to separate target's RCS characters from background in electromagnetic sensing within anechoic chamber measurement," *Green Computing and Communications, IEEE and Internet of Things, IEEE International Conference on and IEEE Cyber, Physical and Social Computing*, 1058–1063, Beijing, 2013.
5. MI Technologies, MI-830 Family of RCS Pylons, Catalog No.: DS-830-1.3/08/13.
6. Orbit/FR, RCS Products, http://www.orbitfr.com/sites/www.orbitfr.com/files/RCS_pylon_brochure.pdf.
7. Knott, E. F., *Radar Cross Section Measurements*, SciTech Publishing, New York, 2006.
8. Lai, A. K.-Y. and M. D. Burnside, "A GTD analysis of ogive pedestal," 716148-8, Ohio State University, USA, 1986.
9. Jiao, H.-J., Y.-D. Zhang, and W.-Y. Chen, "The lightweight design of low RCS pylon based on structural bionics," *Journal of Bionic Engineering*, Vol. 7, No. 2, 182–190, 2010.
10. Burns, J., E. Le Baron, and G. Fliss, "Characterization of target-pylon interactions in RCS measurements," *IEEE Antennas and Propagation Society International Symposium*, Vol. 1, 144–147, 1997.
11. Chen, P.-H., X.-J. Xu, and Y.-S. Jiang, "Comparison of methods to extract target scattering from scattering of target-metal pylon combination," *International Radar Conference*, 1–6, Lille, 2014.
12. Kouyoumjian, R. G. and P. H. Pathak, "A uniform geometrical theory of diffraction for an edge in a perfectly conducting surface," *Proc. IEEE*, Vol. 62, No. 11, 1448–1461, 1974.

13. Dassault Systèmes, CATIA V5 R20 Infrastructure User Guide, 2009.
14. ANSYS, Inc., ANSYS Help 14.5, 2012.
15. EM Software & Systems, S.A. (Pty) Ltd., FEKO User's Manual Suite 6.0, 2010.
16. An, D.-W. and W.-Y. Chen, "Simulation approach to calculate the separation error of target and background from metal pylon deformation," *International Conference on Instrumentation, Measurement, Computer, Communication and Control (IMCCC)*, 719–722, 2015.